Wear 338-339 (2015) 155–163

Contents lists available at ScienceDirect

Wear

journal homepage: www.elsevier.com/locate/wear

Enhanced approach of assessing the corrosive wear of engineering materials under impingement

L. Giourntas [a,*], T. Hodgkiess [b], A.M. Galloway [a]

[a] *Department of Mechanical and Aerospace Engineering, University of Strathclyde, Glasgow, Scotland*
[b] *Porthan Limited, Lochgilphead, Scotland*

ARTICLE INFO

Article history:
Received 26 January 2015
Received in revised form
22 May 2015
Accepted 1 June 2015
Available online 10 June 2015

Keywords:
Corrosive wear
Sliding abrasion
Electrochemical monitoring
Jet impingement

ABSTRACT

Corrosive wear phenomena are apparent in hydraulic machinery that handle slurries. This study focuses on the development of an integrated methodology of material assessment that is employed to understand the mechanisms of deterioration and effectively compare materials' performance under impinging slurry. The technique involves gravimetric measurements and post-test analysis of the surface, which comprises measurement of wear scar depths and volumes, that yield the quantification of the various material degradation processes that occur directly under, and adjacent to, the impinging jet. A medium carbon steel and a stainless steel have been investigated, since they exhibit different corrosive wear behaviour.

1. Introduction

In a wide range of industrial situations, problems arise when a stream of water impinges on, or flows over, components. The consequent deterioration process is, of course, exacerbated when the aqueous fluid is severely corrosive and also when it contains suspended particles that may range in size from fine sand through to large mineral particles. Methods of combating the erosion–corrosion phenomena, understandably, have attracted a substantial interest in the research community where relevant factors associated both with the environmental parameters and materials/coatings performance has been intensively investigated.

A number of experimental techniques have been adopted for study of these types of corrosive wear of which the most common appears to be the submerged jet apparatus [1,2], but other important methods are slurry pot [3], Coriolis [4,5] and rotating cylinder [6]. Approaches that involve mapping of the inter-relationship between erosion corrosion damage and environmental parameters, have also been utilised [7,8]. Another desirable approach involves mathematical modelling of corrosive wear which often makes use of CFD packages to predict flow regimes [9,10]. Although there have been some interesting studies, for instance focusing on modelling damage immediately under a perpendicularly-impinging slurry [11], there are formidable obstacles to this type of approach when dealing with such a complex phenomenon that involves corrosion processes and interactive events. Thus, at present at least, it is evident that the main thrust of research into corrosive wear must depend on experimental investigations.

The focus of the present paper is the most widely-used experimental technique; submerged jet. In such experiments, an aqueous stream, with or without solid particles, is directed onto a specimen whose surface area is greater than the diameter of the jet. The great majority of test programmes have adopted a 90° angle of impingement – although, of course, industrial equipment is subject to a range of angles [12].

Some studies have investigated the effect of angle of impingement in pure erosion conditions [13–15], where the classical theories [16] of the mechanical damage mechanisms are relevant. Other researchers have assessed also the erosion–corrosion behaviour over a range of impingement angles [1,17].

A basic feature of all jet impingement tests is that they involve a measurement of the specimen mass loss and such information has proved valuable in exercises that compare different materials or test conditions. It should be recognised, however, that the total mass loss of a specimen, which is subjected to a typical submerged jet, is a measure of damage in two distinct regions;

- The directly impinged zone in which a distinct wear scar is produced.
- The surrounding area over which the fluid is producing an essentially abrasive action.

---

* Corresponding author.
E-mail address: lampros.giourntas@strath.ac.uk (L. Giourntas).

http://dx.doi.org/10.1016/j.wear.2015.06.004
0043-1648/

Whilst it is well-known that the localised damage is more severe in the directly impinged zone, the material loss is unlikely to be negligible in the area outwith the wear scar. Moreover, a change in target material, or impinging fluid characteristics, might result in differing relative magnitudes of damage in those two regions.

It is apparent, therefore, that the output from investigations that employ the submerged jet technique would be enhanced by post-test evaluation that included unravelling of the total mass loss into the two separate components of damage. This strategy will contribute to a deeper interpretation of fundamental mechanisms of corrosive wear and expanded data for industrial use. This is a tactic that, to the authors' knowledge, does not appear to have been employed hitherto. The key inspection method that will contribute to this objective is surface profiling/topography. There are several ways of undertaking topographical investigations; Atomic force microscopy (AFM), Interferometry, Stylus, and optical profilometry. The simplest type of profiling is the line scan across a specimen surface which yields wear scar depths. Only a few research papers quote such measurements and, in any case, this approach does not directly provide the most desired information [4,11,18]. One such study did briefly involve an estimation of wear scar volume by employing solid geometry to measure values of wear scar depth and diameter on commercially-pure titanium alloy specimen after erosion corrosion [19]. Clearly, the optimum way of obtaining the wear scar volume is from 3-D surface profiling. Occasionally papers show such a 3-D image of a specimen after testing but do not quote any volumes resulting from the image [20]. One piece of work did measure the wear scar volumes of API X42 steel which had been subjected to dry sand erosion [14]. Other researchers appear to have addressed the issue of comparing mass losses within the wear scar with the overall mass loss but within the focused context of corrosion inhibitor performance with limited data being presented [21].

The objective of the work described in the present paper was to extend the conventional scope of jet impingement test evaluation in order to obtain the additional information that is discussed above. To broaden this assessment, experiments were conducted on two steel alloys (a carbon steel and a stainless steel) that would be expected to behave rather differently in erosion corrosion conditions.

2. Methodology

The steels that were selected for this study are listed below:

- Austenitic stainless steel (UNS S31600), which exhibits good corrosion resistance in various corrosive environments.
- A medium carbon steel (UNS G10400), which has poor corrosion performance in most aqueous conditions.

Their typical compositions, as well as their hardness measured, on a Vicker's hardness machine with 5 kgf, are shown in Table 1.

Mass loss measurements were carried out under solid/liquid impingement in free erosion–corrosion conditions, which represents real life operational conditions. Also, experiments were carried out involving the application of cathodic protection to the impinged specimen in order to provide an assessment of the potential benefits that could accrue from the use of this corrosion control technique and also to provide information about the mechanical deterioration mechanisms of the steels. Also, post-experimental analysis was facilitated with Alicona InfiniteFocus equipment with sensitivity of ±1 μm on wear scar depths and $\pm 0.02\ \text{mm}^3$ on wear scar volumes.

The erosion–corrosion experiments were carried out using a circulating closed loop rig (Fig. 1). The duration of the tests was 1 h. The nozzle diameter was 3 mm and the slurry, which consisted of 3.5% NaCl and sand particles, impinged at 19 m/s velocity perpendicular to the specimen surface. The silica sand particles used in this study possess hardness of 1160HV with spherical shape, as shown in Fig. 2. The sand concentration, which was measured directly under the nozzle, was 150 mg/l. Table 2 represents the sand particle size distribution. The testing temperature range was 30–36 °C. The specimens were ground on 220, 500, 800, and 1200 SiC grit papers. The distance between the specimens and the nozzle was fixed at 5 mm. A mass balance of accuracy 0.1 mg was used for the mass loss measurements. After the free erosion–corrosion experiments, the medium carbon steel specimens were immersed briefly in an inhibited acid solution (Clark's solution) before weighing due to the extensive corrosion on their surface.

The evolution of the specimen electrode potential, E_{corr}, (or open circuit potential) was assessed during a one-hour test. Full DC anodic potentiodynamic polarisation scans started after 15 min, to allow the E_{corr} to settle down, by shifting the potential of the test from 20 mV more negative to E_{corr}, to more positive potentials (about 300 mV above E_{corr}) at a fixed sweep rate of 14 mV/min. The potential range of each polarisation scan was sufficient to facilitate corrosion current determination via Tafel extrapolation. The anodic polarisation scans were conducted initially on full specimens. To gain a better understanding of the electrochemical processes that occur on each region, anodic polarisation scans were also undertaken on segmented specimens, the configuration of which is shown in Fig. 3. The segmented

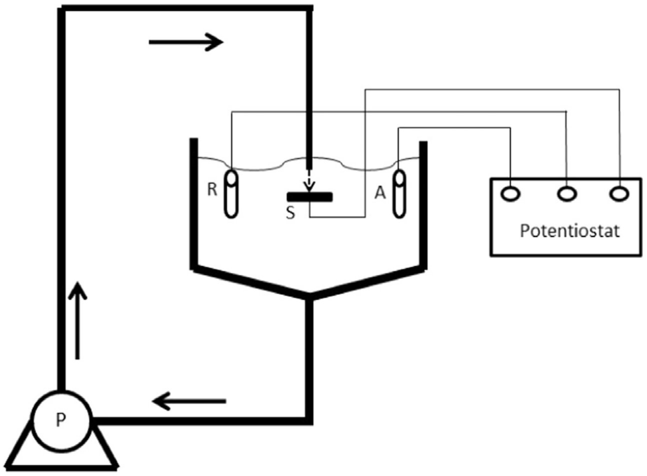

Fig. 1. Schematic diagram of solid/liquid jet impingement circulating rig showing electrochemical equipment (A – Auxiliary Electrode, R – Reference Electrode, S – Specimen (Working Electrode)).

Table 1
Typical composition and hardness of the steels.

Material	C%	Cr%	Ni%	Mo%	S%	Mn%	Si%	N%	P%	Hardness (HV)
UNS S31600	≤ 0.08	16–18	10–14	2.0–3.0	≤ 0.03	≤ 2.0	≤ 0.75	≤ 0.1	0.045	200
UNS G10400	0.37–0.44				≤ 0.05	0.6-0.9			≤ 0.04	240